A Greedy Approach for mmWave Hybrid Precoding with Subarray Architectures

Marcin Iwanow*†, Nikola Vučić*, Samer Bazzi*, Jian Luo*, Wolfgang Utschick†
*Huawei Technologies, German Research Center, Munich, Germany
Email: {iwanow.marcin, nikola.vucic, samer.bazzi, jianluo}@huawei.com
†Associate Institute for Signal Processing, Technische Universität München (TUM), Germany
Email: utschick@tum.de

***Abstract*—We consider a point-to-point mmWave link with hybrid digital-analog transceivers, where the analog stage is realized with a network of phase shifters. Moreover, we concentrate on a case particularly relevant from the practical perspective. Namely, we constrain the analog stage such that disjoint antenna subarrays are processed separately in the analog domain.**

In this work, a novel precoding and combining strategy is developed. In order to exploit the inherent modularity of the analog stage in the subarray architectures, we separate the design of the digital and analog processing and concentrate on the latter. Namely, for the design of the analog stage we propose a subspace-arrangement based greedy algorithm.

I. Introduction

In order to account for limited scattering and small antenna apertures at the mmWave frequencies, a large number of antennas at both sides of the link is required. However, providing an RF chain (consisting, i.a., of the analog-to-digital/digital-to-analog converter (ADC/DAC), up(down)converter, power amplifier) for all antennas is infeasible for a number of reasons. The perhaps most important one is the power consumption of high resolution ADC/DACs. One idea of overcoming this issue is to limit the number of RF chains and introduce an analog circuit between them and the antennas. The circuit effectively acts as a linear map between a large dimension space determined by the number of antennas and a low dimension space defined by the number of available RF chains. Such architecture is usually referred to as hybrid analog-digital.

Early works on the hybrid analog-digital architecture assumed realization of the analog circuit with a network of phase shifters interconnecting every RF chain with each antenna, like depicted in Fig. 1a. Such an architecture requires a design of an overly complex analog circuit. We refer to it as fully interconnected hybrid beamforming (FI-HBF).

A practical implementation of the analog circuit requires dividing the antenna array into subarrays. Each subarray is processed separately by a network of power dividers, combiners, and phase shifters, as shown in Fig 1b. In mathematical sense, the matrix providing the linear map between the antennas and the RF chains ($\boldsymbol{P}_A$ at the transmitter (Tx) and $\boldsymbol{G}_A$ at the receiver (Rx)) becomes block diagonal. We refer to such architecture as subarray partially interconnected hybrid beamforming (SPI-HBF).

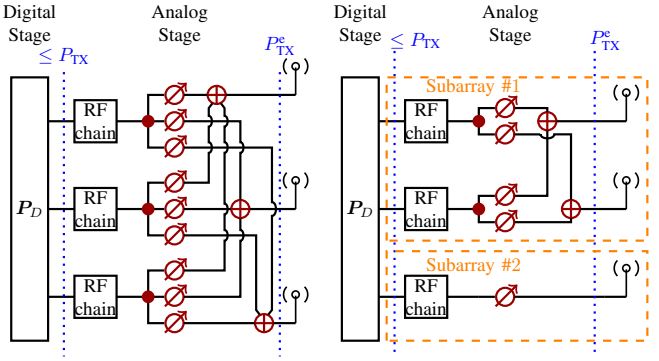

(a) Exemplary FI-HBF transmitter structure. (b) Exemplary SPI-HBF transmitter structure.

Fig. 1. Comparison of the (a) fully and (b) partially interconnected hybrid transmitter structure. The structure of the receiver is similar, with exchanged combiners $\oplus$ and signal splitters $\bullet$.

The design of the analog processing boils down to steering the phase shifters, equivalently choosing the phases of the fixed-magnitude entries of $\boldsymbol{P}_A$ and $\boldsymbol{G}_A$. Unfortunately, the optimal design in the sense of maximizing the achievable rate is an intricate problem.

A. Contribution

We extend the algorithm presented in [1] to a multiuser scenario.

II. System and Channel Model

We consider a single Tx-Rx link, where both transceivers have the SPI-HBF architecture. We call $\boldsymbol{P}_A$ and $\boldsymbol{G}_A$ the analog precoding and combining matrices, respectively. The linear processing at the baseband of Tx and Rx is performed by the digital precoding and combining matrices, denoted by $\boldsymbol{P}_D$ and $\boldsymbol{G}_D$, respectively. Consequently, the recovered version of the transmitted symbol vector $\boldsymbol{s} \sim \mathcal{N}_{\mathbb{C}}(\boldsymbol{0}, \boldsymbol{I})$ reads

$$\hat{\boldsymbol{s}} = \boldsymbol{G}_D^{\text{H}} \boldsymbol{G}_A^{\text{H}} (\boldsymbol{H} \boldsymbol{P}_A \boldsymbol{P}_D \boldsymbol{s} + \boldsymbol{\eta}) \tag{1}$$

where $\boldsymbol{\eta} \sim \mathcal{N}_{\mathbb{C}}(0, \boldsymbol{R}_\eta)$ is a Gaussian noise at the receiver and $\boldsymbol{H}$ is the narrowband channel between the Tx and the Rx.

Following the conclusions from mmWave channel measurement campaigns, we assume the clustered geometric channel model. From the path gains, the direction of arrival/departure

for each path and the corresponding antenna response vectors at the Tx and Rx, we construct the narrowband channel as follows

$$\boldsymbol{H} = \sqrt{\frac{N_{\text{RX}}^{\text{ant}} N_{\text{TX}}^{\text{ant}}}{\sum_{l=1}^{N_{\text{cl}}} N_{\text{path}}^{l}}} \sum_{l=1}^{N_{\text{cl}}} \sum_{r=1}^{N_{\text{path}}^{l}} \alpha_{r,l} \boldsymbol{a}_{\text{RX}}(\theta_{r,l}^{\text{RX}}) \boldsymbol{a}_{\text{TX}}^{\text{H}}(\theta_{r,l}^{\text{TX}}). \quad (2)$$

where N_{cl} is the number of clusters, N_{path}^{l} is the number of paths in the l-th cluster, $\alpha_{r,l}$ is the path gain, $\theta_{r,l}^{\text{RX}}$ and $\theta_{r,l}^{\text{TX}}$ are the angles of arrival (AoA) and departure (AoD), respectively. The vectors $\boldsymbol{a}_{\text{RX}} \in \mathbb{C}^{N_{\text{RX}}^{\text{ant}}}$ and $\boldsymbol{a}_{\text{TX}} \in \mathbb{C}^{N_{\text{TX}}^{\text{ant}}}$ are compound antenna array response vectors for the receiver and the transmitter, respectively which contain concatenated array response vectors of all the subarrays. We assume that the subarrays together form a uniform linear array (ULA) with half-wavelength antenna spacing and therefore the array response vectors have the form

$$\boldsymbol{a}_{\text{ULA}}(\theta) = \frac{1}{N_{\text{ant}}} \left[1, e^{j\pi \sin(\theta)}, \ldots, e^{j(N_{\text{ant}}-1)\pi \sin(\theta)}\right]. \quad (3)$$

We assume perfect knowledge of the channel matrix at both the RX and TX, leaving the analysis for imperfect channel for further work.

III. Proposed Solution

A. Problem Description

We use the achievable rate as the performance measure and write it as

$$R_A = \log_2 \det\left(\boldsymbol{I} + \boldsymbol{R}_{\eta_{\text{eff}}}^{-1} \boldsymbol{H}_{\text{eff}} \boldsymbol{H}_{\text{eff}}^{\text{H}}\right) \quad (4)$$

where $\boldsymbol{H}_{\text{eff}} = \boldsymbol{G}_D^{\text{H}} \boldsymbol{G}_A^{\text{H}} \boldsymbol{H} \boldsymbol{P}_A \boldsymbol{P}_D$ and $\boldsymbol{R}_{\eta_{\text{eff}}} = \boldsymbol{G}_D^{\text{H}} \boldsymbol{G}_A^{\text{H}} \boldsymbol{R}_\eta \boldsymbol{G}_A \boldsymbol{G}_D$. The problem of maximizing R_A with respect to the analog/digital precoders and combiners reads

$$R_A^\star = \max_{\boldsymbol{P}_A, \boldsymbol{G}_A, \boldsymbol{P}_D, \boldsymbol{G}_D} R_A \quad (5)$$

Unfortunately, is very involved. On the other hand, the problem is convex and has a well known waterfilling solution when $\boldsymbol{P}_A$ and $\boldsymbol{G}_A$ are fixed. Therefore, unlike the strategies inherited from the research on FI-HBF, we do not optimize $\boldsymbol{P}_A$ jointly with $\boldsymbol{P}_D$ but we decouple the optimization into two steps. Namely, in our work we focus on the heuristic design of $\boldsymbol{P}_A$ and $\boldsymbol{G}_A$, i.e., on the inner maximization problem in the relaxed version of the optimization problem in (5), which reads

$$R_{A,\text{relaxed}}^\star = \max_{\boldsymbol{P}_D, \boldsymbol{G}_D} \max_{\boldsymbol{P}_A, \boldsymbol{G}_A} R_A. \quad (6)$$

This can be viewed as constructing a "good" starting point for finding a local optimum.

The matrices $\boldsymbol{P}_A$ and $\boldsymbol{G}_A$ are block diagonal, and the zeros in the matrix represent lack of connection between a specific (antenna, RF chain) pair. Each block represents analog processing of a specific subarray, and we write

$$\boldsymbol{P}_A = \begin{bmatrix} \boldsymbol{P}_A^{(1)} & \boldsymbol{0} & \ldots & \boldsymbol{0} \\ \boldsymbol{0} & \boldsymbol{P}_A^{(2)} & \ddots & \\ \vdots & \ddots & \ddots & \boldsymbol{0} \\ \boldsymbol{0} & & \boldsymbol{0} & \boldsymbol{P}_A^{(S_{\text{Tx}})} \end{bmatrix} \quad (7)$$

where S_{Tx} denotes the number of subarrays at the Tx. $\boldsymbol{G}_A$ is constructed analogously. We assume w.l.o.g that the number of RF chains at the Tx and Rx is equal and denote it with N_{RF}.

The structure suggests a similarity to a multiuser scenario, where the subarrays act as users (cf. [2]). As the subarrays are within one device, they can perfectly share information about the channel and the transmission strategies, but in our architecture they are unable of jointly coding the information.

B. Detailed Algorithm Description

The solution we present in the remainder draws from the idea of successive stream allocation applied by the LISA algorithm [3], [4]. More specifically, in each step i we select a pair of subarrays (k_i, l_i) and corresponding precoding/combining vectors $\boldsymbol{g}_i, \boldsymbol{p}_i$ which maximize the gain of the stream within the available signal subspace. If the effective channel $\boldsymbol{H}_{\text{eff}}^A = \boldsymbol{G}_A^{\text{H}} \boldsymbol{H} \boldsymbol{P}_A$ is written explicitly as

$$\boldsymbol{H}_{\text{eff}}^A = \begin{bmatrix} \boldsymbol{G}_A^{(1)^{\text{H}}} \boldsymbol{H}_{1,1} \boldsymbol{P}_A^{(1)} & \ldots & \boldsymbol{G}_A^{(1)^{\text{H}}} \boldsymbol{H}_{1,S_{\text{Tx}}} \boldsymbol{P}_A^{(S_{\text{Tx}})} \\ \vdots & \ddots & \\ \boldsymbol{G}_A^{(S_{\text{Rx}})^{\text{H}}} \boldsymbol{H}_{S_{\text{Rx}},1} \boldsymbol{P}_A^{(1)} & \ldots & \boldsymbol{G}_A^{(S_{\text{Rx}})^{\text{H}}} \boldsymbol{H}_{S_{\text{Rx}},S_{\text{Tx}}} \boldsymbol{P}_A^{(S_{\text{Tx}})} \end{bmatrix}$$

this corresponds to solving in the i-th step a following optimization problem

$$\{k_i, l_i, \boldsymbol{g}_i, \boldsymbol{q}_i\} = \arg \max_{k,l,\boldsymbol{g},\boldsymbol{q}} |\boldsymbol{g}^{\text{H}} \boldsymbol{\Pi}_k^{(i)} \boldsymbol{H}_{k,l} \boldsymbol{\Xi}_l^{(i)} \boldsymbol{p}|. \quad (8)$$

Such problem is simple to solve and the maximal gain $\sigma = |\boldsymbol{g}_i^{\text{H}} \boldsymbol{\Pi}_{k_i}^{(i)} \boldsymbol{H}_{k_i,l_i} \boldsymbol{\Xi}_{l_i}^{(i)} \boldsymbol{p}|$ corresponds to the largest singular value amongst all $S_{\text{Tx}} S_{\text{Rx}}$ matrices $\boldsymbol{\Pi}_k^{(i)} \boldsymbol{H}_{k,l} \boldsymbol{\Xi}_l^{(i)}$. The $\boldsymbol{\Pi}_k^{(i)}$ and $\boldsymbol{\Xi}_l^{(i)}$ are projection matrices onto the column and row spaces of $\boldsymbol{H}_{k,l}$, respectively, and are updated in each step of the algorithm starting from $\boldsymbol{\Pi}_k^{(0)} = \boldsymbol{I}, \boldsymbol{\Xi}_l^{(0)} = \boldsymbol{I}$ for all k, l. We note that complete inter-stream interference mitigation means enforcing

$$\forall i \neq j \implies \boldsymbol{g}_i^{\text{H}} \boldsymbol{H}_{k_i,l_j} \boldsymbol{p}_j = 0$$

which corresponds to diagonalization of $\boldsymbol{H}_{\text{eff}}^{A}$. This is possible by updating the projectors in the i-th step as follows

$$\begin{aligned}
&\forall (k,l) \in \{1,\dots,S_{\text{Rx}}\} \times \{1,\dots,S_{\text{Tx}}\} \\
&\quad \boldsymbol{v}_l^{\text{H}} = \boldsymbol{g}_i^{\text{H}} \boldsymbol{H}_{k_i,l} \boldsymbol{\Xi}_t^{(i)} \\
&\quad \boldsymbol{v}_k = \boldsymbol{\Pi}_r^{(i)} \boldsymbol{H}_{k,l_i} \boldsymbol{p}_i \\
&\boldsymbol{\Xi}_l^{(i+1)} = \boldsymbol{\Xi}_l^{(i)} - \boldsymbol{v}_l (\boldsymbol{v}_l^{\text{H}} \boldsymbol{v}_l)^{-1} \boldsymbol{v}_l^{\text{H}} \\
&\qquad\qquad = \boldsymbol{\Xi}_l^{(i)} - \frac{\boldsymbol{v}_l \boldsymbol{v}_l^{\text{H}}}{\|\boldsymbol{v}_l\|_2^2}, \qquad (9) \\
&\boldsymbol{\Pi}_k^{(i+1)} = \boldsymbol{\Pi}_k^{(i)} - \frac{\boldsymbol{v}_k \boldsymbol{v}_k^{\text{H}}}{\|\boldsymbol{v}_k\|_2^2}. \qquad (10)
\end{aligned}$$

The projectors orthogonally project out the space corresponding to the currently allocated stream, both at the Rx and Tx.

Such conservative zero-forcing approach can often be a wrong choice as it significantly reduces the degrees of freedom (in this case, the remaining subspace) for allocating the consecutive streams. This is expected to be especially pronounced in the mmWave frequencies, where the channel experiences limited scattering.

On the other hand, a significant portion of interference is suppressed if in the i-th step only $\boldsymbol{\Xi}_{l_i}^{(i)}$ and $\boldsymbol{\Pi}_{k_i}^{(i)}$ are updated, which can be written as following

$$\begin{aligned}
\boldsymbol{v}^{\text{H}} &= \boldsymbol{g}_i^{\text{H}} \boldsymbol{H}_{k_i,l_i} = \sigma \boldsymbol{p}_i^{\text{H}} \\
\boldsymbol{\Xi}_{l_i}^{(i+1)} &= \boldsymbol{\Xi}_{l_i}^{(i)} - \boldsymbol{v} (\boldsymbol{v}^{\text{H}} \boldsymbol{v})^{-1} \boldsymbol{v}^{\text{H}} \\
&= \boldsymbol{\Xi}_{l_i}^{(i)} - \boldsymbol{p}_i \boldsymbol{p}_i^{\text{H}} \\
\boldsymbol{\Pi}_{k_i}^{(i+1)} &= \boldsymbol{\Pi}_{k_i}^{(i)} - \boldsymbol{g}_i \boldsymbol{g}_i^{\text{H}}. \qquad (11)
\end{aligned}$$

It can be easily verified that with such construction, following is enforced

$$j > i \wedge k_j = k_i \implies \boldsymbol{g}_j^{\text{H}} \boldsymbol{H}_{k_j,l_i} \boldsymbol{p}_i = 0 \qquad (12)$$

$$j > i \wedge l_j = l_i \implies \boldsymbol{g}_i^{\text{H}} \boldsymbol{H}_{k_i,l_j} \boldsymbol{p}_j = 0 \qquad (13)$$

In other words, the already allocated streams do not *interfere* other streams allocated later to the same Rx subarray (12) and do not *experience interference* from streams later allocated to the same Tx subarray (13).

In the end, we describe how to manage the number of streams in case the digital precoder $\boldsymbol{P}_D$ performs uniform power allocation. Allocation of N_{RF} streams would maximize the achievable rate only in the high SNR region. However, the construction of $\boldsymbol{P}_A$ does not allow to terminate the operation if allocating a new stream does not provide any more gain. Alternatively, we propose to repeat the allocation of the "last" stream, if the corresponding Tx and Rx subarrays still have RF chains available. Such operation increases the gain of the already allocated stream.

The details of the solutions are presented in Algorithm 1. We note that the construction of the projection matrices $\boldsymbol{\Pi}^{(i)}$ and $\boldsymbol{\Xi}^{(i)}$ has not been specified, as the best choice can vary dependent on the particular setup and channel. With $R(\boldsymbol{P}_A^{\star}, \boldsymbol{G}_A^{\star})$ we write the maximal rate achievable with analog precoder $\boldsymbol{P}_A^{\star}$ and analog combiner $\boldsymbol{G}_A^{\star}$, if $\boldsymbol{P}_D$ allocates power uniformly among the streams. We note that in case the transmitter can perform optimal waterfilling precoding, lines 5-17 should be omitted.

Algorithm 1 Successive stream allocation for SPI-HBF with uniform power allocation

1: **Inputs:**
   $\boldsymbol{H}$
2: **Initialize:**
   $\forall k \in \{1,\dots,S_{\text{Rx}}\}, l \in \{1,\dots,S_{\text{Tx}}\}$
   $\boldsymbol{G}_A^{(k)} \leftarrow$ Null, $\boldsymbol{P}_A^{(l)} \leftarrow$ Null
   $\boldsymbol{\Xi}_l^{(1)} \leftarrow \boldsymbol{I}$, $\boldsymbol{\Pi}_k^{(1)} \leftarrow \boldsymbol{I} \quad \forall l,k$
3: **for** $i = 1,\dots,N_{\text{RF}}$ **do**
4: $\{k_i, l_i, \boldsymbol{g}_i, \boldsymbol{p}_i\} = \arg\max_{k,l,\boldsymbol{g},\boldsymbol{p}} |\boldsymbol{g}^{\text{H}} \boldsymbol{\Pi}_k^{(i)} \boldsymbol{H}_{k,l} \boldsymbol{\Xi}_l^{(i)} \boldsymbol{p}|$
   Notes: (1) exclude the subarrays with no more RF chains available (2) $\|\boldsymbol{g}\| = \|\boldsymbol{p}\| = 1$

   Decide whether to add a new stream

   Calculate the rate after the stream allocation

5: $\boldsymbol{G}_{\text{ns}} = \left[\boldsymbol{G}_A^{(k_i)} \boldsymbol{g}_i\right], \quad \boldsymbol{P}_{\text{ns}} = \left[\boldsymbol{P}_A^{(l_i)} \boldsymbol{p}_i\right]$
6: $\boldsymbol{G}_{A,\text{ns}} = \text{diag}(\boldsymbol{G}_A^{(1)}, \dots, \boldsymbol{G}_A^{(k_i-1)}, \boldsymbol{G}_{\text{ns}}, \dots, \boldsymbol{G}_A^{(S_{\text{Rx}})})$
7: $\boldsymbol{P}_{A,\text{ns}} = \text{diag}(\boldsymbol{P}_A^{(1)}, \dots, \boldsymbol{P}_A^{(l_i-1)}, \boldsymbol{P}_{\text{ns}}, \dots, \boldsymbol{P}_A^{(S_{\text{Tx}})})$
8: $R_{\text{ns}} = R(\boldsymbol{P}_{A,\text{ns}}, \boldsymbol{G}_{A,\text{ns}})$

   Calculate the rate, if current RF chain is used to increase the gain of the previous stream

9: $\boldsymbol{G}_{\text{rs}} = \left[\boldsymbol{G}_A^{(k_{i-1})} \boldsymbol{g}_{i-1}\right], \quad \boldsymbol{P}_{\text{rs}} = \left[\boldsymbol{P}_A^{(l_{i-1})} \boldsymbol{p}_{i-1}\right]$
10: $\boldsymbol{G}_{A,\text{rs}} = \text{diag}(\boldsymbol{G}_A^{(1)} \dots \boldsymbol{G}_A^{(k_{i-1}-1)}, \boldsymbol{G}_{\text{rs}}, \dots, \boldsymbol{G}_A^{(S_{\text{Rx}})})$
11: $\boldsymbol{P}_{A,\text{rs}} = \text{diag}(\boldsymbol{P}_A^{(1)} \dots \boldsymbol{P}_A^{(l_{i-1}-1)}, \boldsymbol{P}_{\text{rs}}, \dots, \boldsymbol{P}_A^{(S_{\text{Tx}})})$
12: $R_{\text{rs}} = R(\boldsymbol{P}_{\text{rs}}, \boldsymbol{G}_{\text{rs}})$

13: **if** $R_{\text{rs}} > R_{\text{ns}}$ and subarrays k_{i-1}, l_{i-1} still have available RF chains **then**
14: $\boldsymbol{g} = \boldsymbol{g}_{i-1}$, $\boldsymbol{p} = \boldsymbol{p}_{i-1}$, $k = k_{i-1}$, $l = l_{i-1}$
15: **else**
16: $\boldsymbol{g} = \boldsymbol{g}_i$, $\boldsymbol{p} = \boldsymbol{p}_i$, $k = k_i$, $l = l_i$
17: **end if**
18: $\boldsymbol{G}_A^{(k)} = \left[\boldsymbol{G}_A^{(k)}, \boldsymbol{g}\right], \quad \boldsymbol{P}_A^{(l)} = \left[\boldsymbol{P}_A^{(l)}, \boldsymbol{p}\right]$
19: Update $\boldsymbol{\Xi}_l^{(i)}$, $\boldsymbol{\Pi}_k^{(i)} \quad \forall l,k$
20: **end for**
21: Scale the entries of $\boldsymbol{P}_A$ and $\boldsymbol{G}_A$ such that the absolute value of each non-zero entry is appropriate
22: **return** $\boldsymbol{P}_A, \boldsymbol{G}_A$

C. Motivation for the Approach

The motivation for the presented solution is threefold. Firstly, motivated by the MIMO theory, we aim on picking and separating the strongest modes of the channel. Secondly, the freedom of designing the projector matrices $\boldsymbol{\Pi}^{(i)}$ and $\boldsymbol{\Xi}^{(i)}$ allows to control dependency between the chosen modes. For

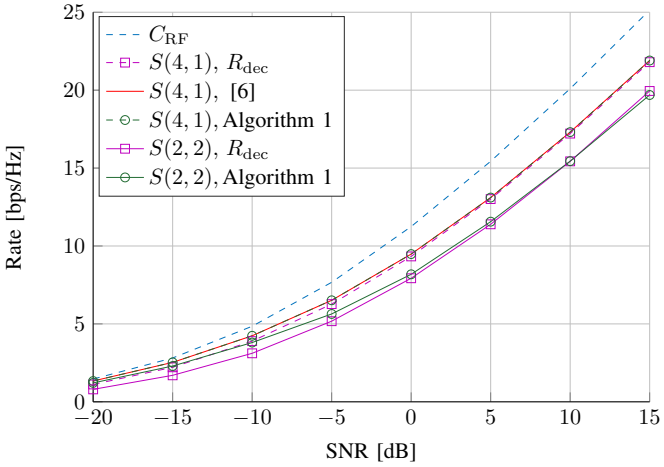

Fig. 2. The performance of the solution compared with a baseline algorithm

the millimeter channel which usually consist of a small number of significant paths, enforcing orthogonal modes by means of zero forcing in the analog stage is too conservative. In Fig. 3, we compare zero forcing (10) with a less conservative approach which allows for a degree of dependency between the streams(11). Whereas for the rich Rayleigh channel the performance gap is small, zero forcing achieves very poor results for the mmWave channel. Finally, the distributed nature and scalability of the algorithm can match different setups of the subarray architecture.

IV. Simulations

In the simulations, we compare the performance of the presented solution with:

- the channel capacity constrained by the number of RF chains (C_{RF}),
- the performance of an algorithm based on the decomposition of the unconstrained precoder/combiner matrices (R_{dec}), like in [5].
- the performance of an algorithm based on the multiuser perspective from [6] (R_{MU}). The algorithm operates only for one subarray at the Rx and one RF chain per subarray at the Tx.

In our simulations, we distribute the RF chains and antennas uniformly among the subarrays and denote with $S(m,n)$ a subarray setup with m subarrays at the Tx and n subarrays at the Rx. The overall number of antennas at the Tx and Rx is 64 and 16, respectively, and $N_{\mathrm{RF}} = 4$. The channel consists of 3 clusters each containing 10 paths.

We note that the algorithm presented in [6] is, for the subarray setup considered therein, a special case of the presented solution and thus provides the same results.

The results show that the algorithm is very promising. It is outperforming the baseline approach in low SNR, as it can allocate lower number of streams than the number of RF chains. In the high SNR regime, the performance is comparable.

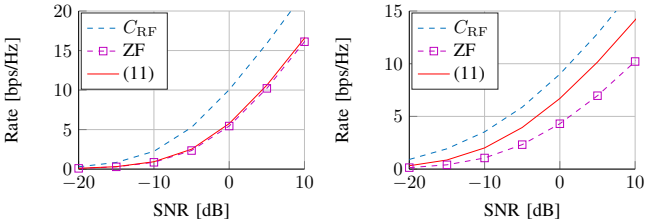

(a) Rayleigh channel (b) mmWave channel

Fig. 3. Comparison of the zero-forcing approach (projector update as in (10)) with the less conservative approach (11) for the Rayleigh and mmWave channel. The simulation parameters are as in Section IV and the subarray configuration is $S(2,2)$.

V. Conclusions

A new way of designing hybrid digital-analog precoding has been presented. Unlike most approaches in the literature, the design of the analog and digital precoders has been decoupled. The results show that it hasn't entailed a sacrifice in the performance.

This is an important outcome, which suggests that decentralized and flexible design of analog precoders does not necessarily imply a loss in performance. The presented method, which can be in short described as sequential arrangement of subspaces has been proved to be successful also for a multiuser mmWave scenario with FI-HBF transceivers [4].

The next step in evaluating the approach should include the evolution to incomplete CSI scenarios and multiuser systems.

References

[1] M. Iwanow, N. Vucic, S. Bazzi, J. Luo, and W. Utschick, "A greedy approach for mmwave hybrid precoding with subarray architectures," in *2017 51th Asilomar Conference on Signals, Systems and Computers*, Nov. 2017.

[2] M. Iwanow, N. Vucic, W. Utschick, M. Castaeda, W. Xu, and J. Luo, "Data rate bound for mmwave hybrid beamforming systems with subarrays," in *2017 IEEE 18th International Workshop on Signal Processing Advances in Wireless Communications (SPAWC) (IEEE SPAWC 2017)*, Sapporo, Japan, Jul. 2017.

[3] C. Guthy, W. Utschick, and G. Dietl, "Low-Complexity Linear Zero-Forcing for the MIMO Broadcast Channel," *IEEE Journal of Selected Topics in Signal Processing*, vol. 3, no. 6, pp. 1106–1117, Dec. 2009.

[4] W. Utschick, C. Stockle, M. Joham, and J. Luo, "Hybrid lisa precoding for multiuser millimeter-wave communications," *IEEE Transactions on Wireless Communications*, vol. PP, no. 99, pp. 1–1, 2017.

[5] X. Yu, J. C. Shen, J. Zhang, and K. B. Letaief, "Alternating minimization algorithms for hybrid precoding in millimeter wave MIMO systems," *IEEE Journal of Selected Topics in Signal Processing*, vol. 10, no. 3, pp. 485–500, Apr. 2016.

[6] X. Gao, L. Dai, S. Han, C. L. I, and R. W. Heath, "Energy-efficient hybrid analog and digital precoding for mmwave MIMO systems with large antenna arrays," *IEEE Journal on Selected Areas in Communications*, vol. 34, no. 4, pp. 998–1009, Apr. 2016.